

passive margins [for example, Maine, maximum = 2.2 cm/year (25)] and mid-ocean ridges [for example, Iceland, maximum = 6.9 cm/year (26)] illustrates the influence of mantle viscosity and tectonic setting on the rate of recovery.

The recent discovery of human remains (9880 ± 50 ¹⁴C years B.P.) in a cave on Prince of Wales Island (27–29) immediately north of the Queen Charlotte Islands (Fig. 1) highlights the potential for eventual discovery of early postglacial human occupation of Gwaii Haanas and the adjacent submerged areas of Hecate Strait. Our evidence for marked paleoenvironmental changes in Gwaii Haanas from late-glacial to mid-Holocene time offers insights into the distribution of habitable landscapes (Figs. 5 and 6) along the northern Northwest Coast. Paleobotanical analyses have demonstrated that the Northwest Coast was suitable for human habitation by 13,000 years B.P. (30, 31). Stone tools found on paleobeach sites confirm human occupation by 9300 ¹⁴C years B.P. (Fig. 6). The lack of evidence for human use of the early postglacial landscape may be largely attributable to the drastic and rapid changes in past sea levels. Gwaii Haanas coastlines dating from 9300 to 9100 years B.P. coincide with those of today, coastlines dated before 9300 are deeply drowned (to –153 m), and those dating from 9100 to 5000 years B.P. are stranded in the rainforest some 15 m above current levels. In this context, it is interesting that the Gwaii Haanas Haida Indian oral history abounds in legends of rapidly rising seas (32).

The sea-level curve (Fig. 4) provides an important tool that enables archaeologists to focus their studies in search of paleobeaches and paleohabitats (33, 34). The opportunity to locate evidence of human activity dating to the period of lowered sea levels may be better some 150 km to the east, along the British Columbia coast, where isostatic dynamics resulted in coeval raised marine deposits now situated >200 m above modern sea level.

REFERENCES AND NOTES

1. J. V. Barrie, K. W. Conway, R. W. Mathewes, H. W. Josenhans, J. M. Johns, *Quat. Int.* **20**, 123 (1993).
2. J. J. Clague, in *Shorelines and Isostasy*, D. E. Smith and A. G. Dawson, Eds. (Institute of British Geographers Spec. Publ. 16, 1983), pp. 321–343.
3. J. L. Luternauer et al., *Geology* **17**, 357 (1989).
4. H. W. Josenhans, D. W. Fedje, K. W. Conway, J. V. Barrie, *Mar. Geol.* **125**, 73 (1995).
5. J. J. Clague, *Can. J. Earth Sci.* **22**, 256 (1985).
6. S. Elias, S. K. Short, C. H. Nelson, H. H. Birks, *Nature* **382**, 61 (1996).
7. The QCI archipelago is known by the indigenous Haida Indians as Haida Gwaii, and the study area in the southern islands is referred to as Gwaii Haanas.
8. K. Anundsen, S. Abella, E. Leopold, M. Stuiiver, S. Turner, *Quat. Res.* **42**, 149 (1994).
9. R. Pienitz, G. Lortie, M. Allard, *Geogr. Phys. Quat.* **45** (no. 2), 155 (1991).

10. H. W. Josenhans and J. Zevenhuizen, *Geological Survey of Canada: Open File Map 3207* (1996).
11. D. W. Fedje, thesis, University of Calgary, Alberta, Canada (1993).
12. J. R. Southon and D. W. Fedje, unpublished data.
13. Table of sample parameters and dates that bracket the interval of marine versus brackish or lacustrine conditions recorded in the piston or vibracore samples. The sill height is shown for sites where the constraining sill depth is shallower than the core site. Many of the ¹⁴C dates were derived from young wood fragments to avoid errors introduced by dating of ancestral wood. Table available to *Science* Online subscribers at www.sciencemag.org/
14. J. R. Southon, D. E. Nelson, J. S. Vogel, *Paleoceanography* **5**, 197 (1990).
15. A. Lotter, B. Ammann, J. Beer, I. Hadjas, M. Sturm, in *The Last Deglaciation: Absolute and Radiocarbon Chronologies*, E. Bard and W. S. Broecker, Eds. (NATO ASI Series, Springer-Verlag, Berlin, 1992), vol. 12, pp. 45–68.
16. B. Kromer and B. Becker, *Radiocarbon* **35**, 125 (1993).
17. T. Goslar et al., *Nature* **377**, 414 (1995).
18. E. Bard, M. Arnold, R. G. Fairbanks, B. Hamelin, *Radiocarbon* **35**, 191 (1993).
19. R. L. Edwards et al., *Science* **260**, 962 (1993).
20. E. Bard et al., *Nature* **382**, 241 (1996).
21. S. Björck et al., *Science* **274**, 1155 (1996).
22. H. W. Josenhans and J. Zevenhuizen, *Geological Survey of Canada: Open File Map 3242* (1996).
23. Composite diagram of core 59 showing the relations between lithology, diatom assemblages, interpreted depositional environments, and ¹⁴C age. The age of marine inundation was plotted against water depth at the core site to develop the sea-level curve. Figure available to *Science* Online subscribers at www.sciencemag.org/
24. R. G. Fairbanks, *Nature* **352**, 637 (1989).
25. W. A. Barnhardt, W. R. Gehrels, D. F. Belknap, J. T. Kelly, *Geology* **23** (no. 4), 317 (1995).
26. O. Ingólfsson, H. Norddahl, H. Haflicason, *Boreas* **24**, 245 (1995).
27. T. H. Heaton, S. L. Talbot, G. F. Shields, *Quat. Res.* **46** (no. 2), 186 (1996).
28. J. E. Dixon, T. H. Heaton, T. E. Fifield, paper presented at the 24th Annual Meeting of the Alaska Anthropological Association, Whitehorse, Yukon Territory, Canada, 9 to 11 April 1997.
29. R. E. Ackerman, T. D. Hamilton, R. Stuckenrath, *Can. J. Anthropol.* **3**, 195 (1979).
30. D. H. Mann and T. D. Hamilton, *Quat. Sci. Rev.* **14**, 449 (1995).
31. R. W. Mathewes, in *The Outer Shores*, G. Scudder and N. Gessler, Eds. (Queen Charlotte Museum Press, Seaside, British Columbia, Canada, 1989), pp. 75–90.
32. J. R. Swanton, *Haida, Texts, Masset Dialect* (Memoir of the American Museum of Natural History, New York, 1908), vol. 10.
33. T. Christensen, *The Gwaii Haanas Archeological Project: Raised Beach Surveys, 1995 Field Report* (unpublished report, Canadian Heritage, Victoria, British Columbia, Canada, 1996).
34. D. W. Fedje, A. P. Mackie, J. B. McSparran, B. Wilson, in *Early Human Occupation of British Columbia*, R. L. Carlsen and L. Palla-Bona, Eds. (Univ. of British Columbia Press, Vancouver, Canada, 1996), pp. 133–151.
35. We thank the officers and crews of the research vessels *Endeavour*, *Vector*, *Tully*, and *Gwaii Haanas*. We thank V. Barrie and K. Conway for facilitating the collection of seismic and vibracore data, subsequent analysis, and helpful discussions. Supported by the Geological Survey of Canada and the Gwaii Haanas National Park Reserve–Haida Heritage site and by the U.S. Department of Education under contract W-7405-Eng-48 to Lawrence Livermore National Laboratory. The paper was reviewed by R. Pickrill and J. Shaw. Geological Survey of Canada contribution number 1996456.

25 March 1997; accepted 19 May 1997

Mid- to Late Pleistocene Ice Drift in the Western Arctic Ocean: Evidence for a Different Circulation in the Past

Jens F. Bischof and Dennis A. Darby

The provenance of ice-rafted debris (IRD) in four Arctic sediment cores implies that icebergs from the northwestern Laurentide ice sheets drifted across the western Arctic Ocean along the 180°–0° meridian toward Fram Strait during mid- to late Pleistocene deglaciations within the last 700,000 years. This iceberg drift was different from the present-day Beaufort Gyre circulation and resembled a dislocated transpolar drift (TPD). Sea ice mainly followed the iceberg trajectories but also frequently drifted from the Russian shelves eastward into the Amerasian Basin.

The motion of sea ice in the Arctic Ocean is defined by the Beaufort Gyre, a clockwise circulation in the western Arctic Ocean, and by the TPD in the eastern Arctic Ocean, where ice drifts directly eastward into the Greenland Sea (Fig. 1) (1). As a consequence, ice in the Beaufort Gyre can remain in the Amerasian Basin for decades,

whereas ice in the TPD leaves the Arctic in generally less than 3 years. Little is known about the history of the Beaufort Gyre, which should have homogenized the IRD within the Amerasian Basin. Here, we used data from a petrographic and geochemical analysis of IRD to show that the directions of the ice drift were highly variable during the last 700,000 years and were mostly different from those of today.

The provenance of IRD was determined for four sediment cores—F214, F280, F436, and F542—in the western Arctic Ocean

Applied Marine Research Laboratory, Department of Oceanography, Old Dominion University, 1034 West 45th Street, Norfolk, VA 23529, USA. E-mail: jfb100r@oduvm.cc.odu.edu (J.F.B.), dad100f@oduvm.cc.odu.edu (D.A.D.).

(Fig. 1). We analyzed the petrographic and mineralogic composition of detrital grains $>250 \mu\text{m}$ and the mineralogy and geochemistry of individual opaque Fe oxide minerals in the 45- to $250\text{-}\mu\text{m}$ range from these cores and in 158 samples from potential source areas around the periphery of the Arctic Ocean (Fig. 1). All cores were sampled by cutting 1-cm slices of sediment from lithologic units M, L, and the upper part of K, except for core F542, which was sampled only to the upper part of unit L (Fig. 2). The chronostratigraphic reference horizon is the Brunhes-Matuyama paleomagnetic boundary (780,000 years ago) in the middle of unit K (2, 3). The western Arctic sediments have generally low sedimentation rates of $\sim 1 \text{ mm per } 1000 \text{ years}$ on average (4). The core samples represent a long-term sediment record of approximately 780,000 years in core F436, 630,000 years in core F214, 710,000 years in core F280, and 560,000 years in core F542 (2, 3, 5).

The source area samples—which consist of glacial surface till and outwash, glaciomarine shelf, and interisland channel sediments—represent the composition of lithic debris that was available from potential source terrains for ice-rafting into the Arctic Ocean. We identified 72 different types of detrital grains $>250 \mu\text{m}$, using optical microscopy, and determined the composition of detrital Fe oxide grains by reflected-light microscopy and electron microprobe (6). We grouped the source area clast compositions and Fe oxide geochemistry data into 18 geographically distinct source groups by clustering and discriminant function analysis (DFA). The core data were then compared with the source groups by DFA. As a test of DFA, we compared the $>250 \mu\text{m}$ grain type data of the core samples assigned to a particular group directly with the data of the source group samples.

The Arctic Ocean glaciomarine core sediments are light yellowish-brown to dark olive-gray sandy-silty mud with variable amounts of coarse, glacial IRD (0.1 to 21% $>250 \mu\text{m}$ and 2 to 54% $>63 \mu\text{m}$). The IRD composition of grains $>250 \mu\text{m}$ is dominated by quartz (57.8% of the grains, averaged for all four cores), carbonate fragments (20.7%), and fragments of multicolored crystalline rocks (18.6%). Clastic sedimentary rocks (2.4%) and cherts (0.5%) are rare. Quartz is most abundant on the central Alpha Ridge (71.3% in core F436). Carbonate is most abundant in core F214, the westernmost core (31.5%), and decreases steadily toward the east (22.4% in F280, 20.5% in F436, and 16.0% in F542). Multicolored crystalline rocks (mostly gneiss) are most abundant in core F542 (40.8%) and aver-

age $<10\%$ in the other cores. These differences show that the circulation in the Arctic Ocean during the last 700,000 years did not homogenize clast types.

The carbonate proportion of the IRD is low in the lower part of unit L of cores F214, F280, and F436 (Fig. 2). It gradually rises in F280 and F436 toward the M-L boundary before dropping again in the middle of unit M. In core F214, the entire interval from the middle of unit L to the upper third of unit M is an uninterrupted carbonate high with percentages over 30%. The peak value is 60% in the upper part of unit L in core F214, and the relative amount of carbonate IRD decreases from the F214 site northeastward. These data imply that carbonate clasts were replaced by increasing amounts of quartz toward the northeast. The percentages of crystalline rocks in cores F214, F280, and F436 rise and fall quasi-in phase with the carbonates but show higher frequency undulations. The IRD composition changes are similar to those in five cores from other parts of the western Arctic Ocean and occur in approximately the same

stratigraphic levels (7).

The most important sources of mid- to late Pleistocene IRD grains $>250 \mu\text{m}$ for the western Arctic Ocean are located in the Canadian Arctic Archipelago. Of 271 analyzed samples, 112 discriminant function classifications were obtained from northern North America and Greenland, as opposed to only 6 from Russia (Fig. 2); 85 determinations point to Arctic Canada, mostly to the carbonate-dominated area of Banks and Victoria islands (57 classifications) and the District of Mackenzie (19 classifications). Core F214 received an almost uninterrupted supply of carbonate-rich IRD from Banks and Victoria islands and parts of the District of Mackenzie from the middle of unit L to the upper part of unit M. The crystalline rock-dominated section in the middle to upper part of unit M in core F542 originated from sources in Ellesmere Island and North Greenland. The core with the greatest proportion of source determinations from Banks and Victoria islands is F214 (84% of all DFA determinations), followed by F280 and F436 (54% and

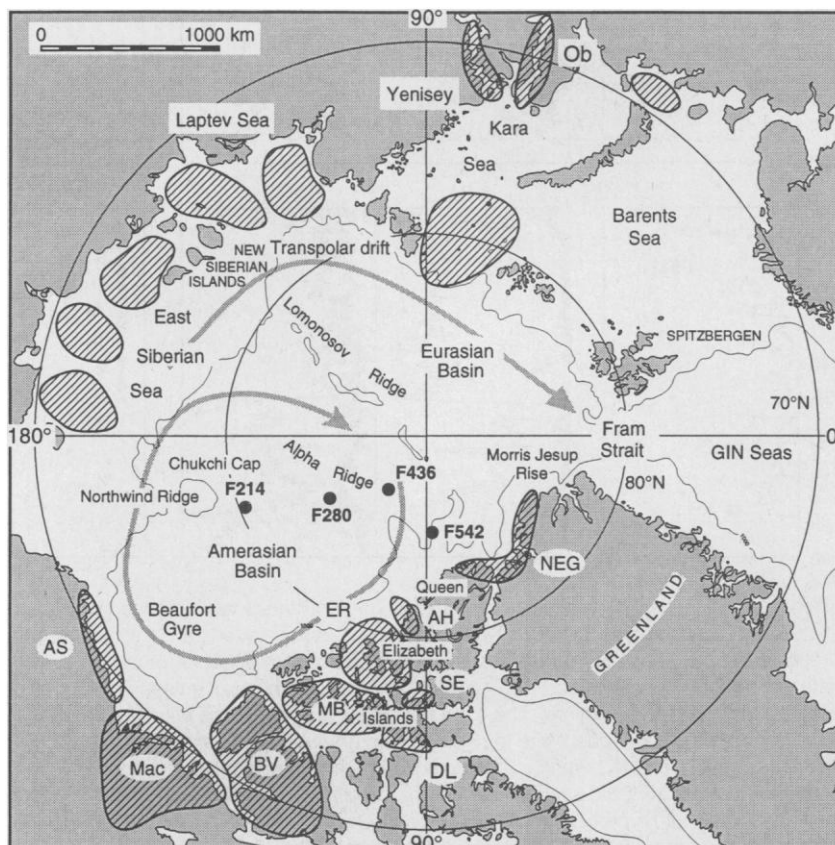


Fig. 1. Map of Arctic Ocean and adjacent landmasses with core locations and 1000-m isobath. Striped areas are source areas defined by clustering and DFA (6). NEG, North Greenland and North Ellesmere Island; AH, Axel Heiberg Island; ER, Ellef Ringnes Island; SE, Southeast Ellesmere Island; DL, Devon Island and Lancaster Sound; MB, Melville and Bathurst Island; BV, Banks and Victoria islands; Mac, Mackenzie Basin and Delta; and AS, Alaska Shelf. Shaded arrows show present ice drift.

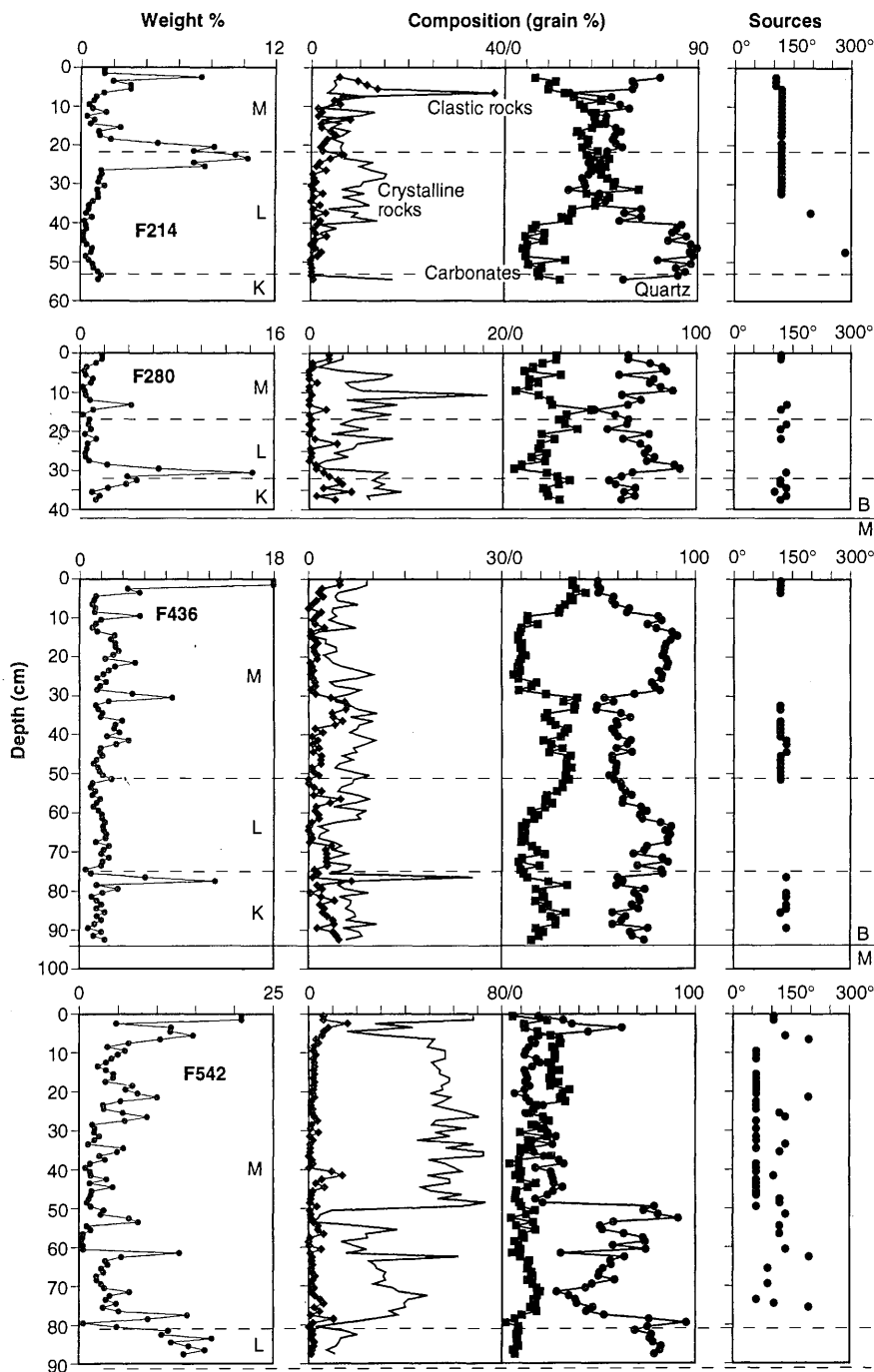


Fig. 2. Downcore variations of the weight percentages, composition, and determined sources of IRD grains $>250 \mu\text{m}$ for each core. There is an inverse relation between quartz and carbonates in cores F214, F280, and F436, but not in F542, where quartz alternates with crystalline rocks. Also, the carbonate percentage curves of cores F214, F280, and F436 show increases and decreases in approximately the same core sections. The carbonate low in the lower part of unit L is recognized in all three cores, as is the subsequent rise to high values at the M-L boundary. This carbonate high is of different thickness and is followed by a drop to minimum values in the middle of unit M in cores F280 and F436, but not in F214, where high carbonate percentages persist until near the core top. Only the IRD sources with a probability of >0.95 are displayed clockwise in degrees longitude from 0° (central Fram Strait) to 300°W (Kara Sea). The sources of the carbonate-rich intervals in cores F214, F280, and F436 are concentrated between 100° and 140°W around the Banks and Victoria islands and in the Mackenzie area. IRD in core F542 mostly originated from North Greenland and northern Ellesmere Island (60° to 80°W), but also from other parts of the Canadian Arctic Archipelago and the Mackenzie area. The two quartz-dominated intervals between 10 and 30 cm and between 60 and 75 cm in F436 are most likely from the western and central Queen Elizabeth Islands. B/M, Brunhes-Matuyama boundary.

67%, respectively). Core F542 was least affected by IRD from Banks and Victoria islands. IRD from North Greenland and Ellesmere Island drifted to the F542 site on the southeastern Alpha Ridge, but not to any of the other three core sites. The conclusion is that IRD from Ellesmere Island and North Greenland drifted only a short distance offshore northward and then turned to the east, toward Fram Strait. The occasional presence of IRD from the Mackenzie area in F542 indicates that, when ice originated from the Mackenzie region, it must have taken a north-eastward route parallel and possibly close to the North American Arctic continental margin.

Most of the 56% misclassifications were obtained for core intervals in which IRD grains $>250 \mu\text{m}$ are almost entirely composed of quartz. The origin of the quartz-rich intervals in F436 between 10 and 30 cm and between 60 and 75 cm, as well as those below 50 cm in F542, remains uncertain but may be from around Ellef Ringnes Island. The composition of grains $>250 \mu\text{m}$ from Ellef Ringnes Island overlaps with those in the eastern Russian Arctic, but DFA of the 20 most abundant IRD lithologies of the quartz-dominated core intervals implies that the Kara Sea is not a source, and that the Ellef Ringnes Island area is a more likely source than are the Ob and Yenisey estuaries. In addition, quartz grains from those rivers are partly covered by a yellowish-red stain, unlike quartz from Ellef Ringnes Island and in our Arctic core IRD.

The most likely sources of Fe oxide IRD are Banks and Victoria islands, the Ellef Ringnes Island region, and northern Russia (Table 1). The data imply that each source contributed fine-grained material equally to all four core locations, in contrast to the $>250\text{-}\mu\text{m}$ fraction. The discrepancy between the sources of the $>250\text{-}\mu\text{m}$ IRD and the 45- to $250\text{-}\mu\text{m}$ Fe oxide grains may be because different types of ice transported different grain size fractions. Large parts of the Laptev Sea, the East Siberian Sea, and the Alaska Shelf were never glaciated (8), and thus the high number of Fe oxide grains from these sources probably represents the portion of the IRD that was rafted by sea ice.

The western Arctic Ocean flux rates of ice-rafted sediment in the cores (0.9 to $2.4 \text{ g m}^{-2} \text{ year}^{-1}$) are lower than those under permanent ice in the East Greenland current ($2.9 \text{ g m}^{-2} \text{ year}^{-1}$) (9), but the Arctic Ocean core sediment is much coarser (11.8 to 21.7 weight % $>63 \mu\text{m}$ on average) than sea ice sediment (0.3 to 1.9 weight %) (10). The sand content of our core samples is more

similar to that of tills from northern Canada (11) than to sea ice sediment. Clark and Hanson (12) calculated that the present-day sediment accumulation rates for particles transported by icebergs would be $15.2 \text{ mg m}^{-2} \text{ year}^{-1}$ for an Arctic Basin of $6.6 \times 10^{12} \text{ m}^2$. Our calculation for the piston core sediment yielded $1.6 \text{ g m}^{-2} \text{ year}^{-1}$ for a sedimentation rate of 1 mm per 1000 years, approximately 100 times the amount that present-day icebergs could produce. Therefore, the sediment accumulation rates of the western Arctic Ocean require more icebergs than exist today, plus some input from sea ice. We conclude that the western Arctic Ocean during the last 700,000 years was permanently ice-covered and that its water temperatures were comparable to or lower than those of today.

The abundance of Fe oxide grains from the Laptev Sea in the western Arctic Ocean also implies that the circulation of sea ice was different from that of today and that the western Arctic Ocean received substantial amounts of sea ice sediment from northern Russia (East Siberian and Laptev seas). This sea ice is largely diverted to the east by the TPD today. The proportions of Fe oxide grains from specific sources change drastically over core intervals of 1 to 3 cm thickness, which indicates that the pattern of ice drift during the mid- to late Pleistocene was variable. The Fe oxide grains also indicate that in every case multiple sources contributed. At most times, more than six sources were providing Fe oxide grains.

On the basis of our IRD composition data and the DFA source determinations, icebergs must have drifted in arcs from the southwestern Canadian Arctic Archipelago and northwest Canada toward the Northwind Ridge and Chukchi Cap area and from the Queen Elizabeth Islands toward the central and southeastern Alpha Ridge during the last 700,000 years, while sea ice drifted from the Siberian shelves toward the western Arctic Ocean with a wind-driven circulation different from that of today (Fig. 3). All of the identified IRD sources in northern Canada and the Canadian Arctic Archipelago, and at times possibly the entire Canadian Arctic Archipelago to the present-day water depth of 300 m, were repeatedly buried under continental and marine-based ice sheets (11, 13–15). Because of the post-glacial isostatic rebound (16), the relative sea level during full glacials was as much as 100 m higher than today, and glacial ice was grounded in water depths of up to 400 m (14). Therefore, icebergs with keel depths of up to 400 m were probably present in the glacial Arctic Ocean. The ice flow shown in Fig. 3 allowed icebergs

Table 1. Sources of Fe oxide grains 45 to 250 μm (as percentages of all classified grains) in the Arctic cores, as determined by DFA.

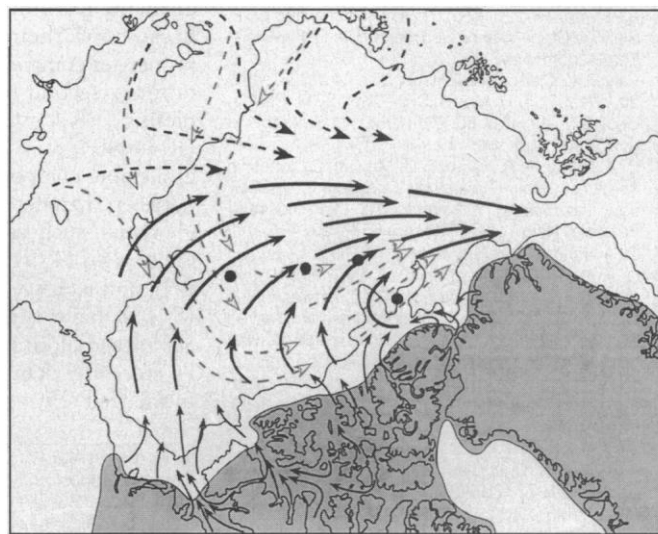
Source	Core composition (grain %)				Total (number of grains)
	F214	F280	F436	F542	
Unknown sources	12.3	13.7	12.9	14.1	1205
Ellesmere Island and North Greenland	4.8	4.1	2.0	5.0	347
Axel Heiberg Island	0.3	–	–	–	3
Ellef Ringnes Island	8.0	8.9	6.9	9.0	732
Southern Queen Elizabeth Islands	9.9	6.2	9.7	6.6	721
Banks and Victoria islands	15.5	18.6	15.0	24.2	1744
District of Mackenzie	3.3	2.8	2.7	1.5	201
Alaska Shelf	7.6	8.4	6.8	7.1	645
East Siberian Sea	17.9	15.4	20.7	12.6	1463
Laptev Sea	16.1	16.1	19.4	15.2	1510
Russia east of Taimyr Peninsula	4.3	5.9	4.0	4.7	408
North America and Greenland	56.4	56.7	49.4	62.2	4393
Canadian Arctic Archipelago	40.3	41.7	37.6	50.0	3400
Northwest Canada	3.7	3.3	3.1	1.7	201
Russian sources	43.6	43.3	50.6	37.8	3381

from the Laurentide and Innuitian ice sheets to exit the Arctic Ocean directly through Fram Strait without multiple rotations in the western Arctic Ocean. This flow pattern is consistent with the dominant wind directions obtained with climate models for the last glacial maximum (17) and is similar to the cyclonic state of periodic changes in the wind-driven circulation during the last 50 years (18). The relatively low sedimentation rates and weight percentages for all coarse grain types $>250 \mu\text{m}$ in the western Arctic Ocean cores F214 and F280 compared with the Alpha Ridge cores F436 and F542 (Fig. 2) are best explained by rapid ice passage across the central western Arctic Ocean, which reduced the amount of time available for particle release from the ice canopy.

The icebergs could not have reentered the Arctic Ocean near Fram Strait because IRD in the eastern Arctic Ocean is different from western Arctic IRD in that it contains primarily siltstones, quartzites, quartz, and feldspar but only minor quantities of carbonates (19), in contrast to the abundance of carbonate clasts in our analyzed cores. Abundant carbonate IRD also has been reported from the western Fram Strait (20) and from the Morris-Jesup Rise north of Greenland (21), in the direction of our postulated flow of ice toward Fram Strait.

Although the sea ice motion is mainly driven by the prevailing winds (22), deep-keeled icebergs are more likely affected by surface currents. Thus, the surface currents within the uppermost several hundred

Fig. 3. Map of the inferred surface current-driven iceberg drift directions from North American sources (solid arrows) and concurrent hypothesized drift of Russian pack ice (broken arrows) during glacial intervals. The sea ice drift in the western Arctic Ocean was mostly similar to the iceberg drift, but sea ice occasionally drifted from Russian sources into the western Arctic Ocean along paths shown as shaded broken arrows. Neither scenario is compatible with the Beaufort Gyre. We infer that relatively fast iceberg passage across the central Arctic Ocean accounts for the lower sedimentation rates and the lower IRD content in that part of the Arctic Ocean.



meters must have been largely similar to the reconstructed iceberg drift tracks. The data suggest that this surface current was driven by an inflow of waters from the south into the Arctic Ocean at deeper levels, probably below 1000 m. This implies that some form of deep-water production similar to the present North Atlantic deep water (NADW) formation must have been operative during glacial periods. It is possible that the formation of NADW never completely stopped during glacial intervals, and that it was modified and occurred in a different part of the northern North Atlantic than today. Evidence for southward-flowing surface currents along the entire width of the Norwegian and Greenland seas during glacial intervals exists from the dispersal of coal fragments of eastern Arctic origin and clastic sedimentary rocks from the Barents Shelf in IRD assemblages of the Norwegian Sea (19, 23). Melting of icebergs from the Laurentide and Innuitian ice sheets in the Greenland-Iceland-Norwegian (GIN) seas could have reduced the surface water salinity and thus affected the NADW formation. This process could have initiated cold glacial conditions and contributed to their maintenance and stabilization.

REFERENCES AND NOTES

1. K. Aagaard and E. C. Carmack, *J. Geophys. Res.* **94**, 14485 (1989); in *The Polar Oceans and Their Role in Shaping the Global Environment: The Nansen Centennial Volume*, O. M. Johannessen, R. D. Muench, J. E. Overland, Eds. (American Geophysical Union, Washington, DC, 1994), pp. 5–20; G. L. Mellor and S. Häkkinen, *ibid.*, pp. 21–31; S. Häkkinen, *J. Geophys. Res.* **98**, 16397 (1993).
2. D. L. Clark, R. R. Whitman, K. A. Morgan, S. D. Mackey, *Geol. Soc. Am. Spec. Pap.* **181** (1980).
3. D. L. Clark, in *The Arctic Ocean Region*, vol. 50 of *The Geology of North America*, A. Grantz, L. Johnson, J. F. Sweeney, Eds. (Geological Society of America, Boulder, CO, 1990), pp. 53–62; H. R. Jackson, P. J. Mudie, S. M. Blasco, Eds., *Geol. Surv. Can. Pap.* **84-22** (1985); D. A. Miniucucci and D. L. Clark, in *Glacial Marine Sedimentation*, B. F. Molnia, Ed. (Plenum, New York, 1983), pp. 331–365; D. K. Pak, D. L. Clark, S. M. Blasco, *Mar. Micropaleontol.* **20**, 1 (1992); T. H. Morris, D. L. Clark, S. M. Blasco, *Geol. Soc. Am. Bull.* **96**, 901 (1985); W. K. Witte and D. V. Kent, *Quat. Res.* **29**, 43 (1988).
4. D. A. Darby, A. S. Naidu, T. C. Mowatt, G. Jones, in *The Arctic Seas, Climatology, Oceanography, Geology, and Biology*, Y. Herman, Ed. (Van Nostrand Reinhold, New York, 1989), pp. 657–720.
5. G. A. Jones, *Polar Res.* **5**, 309 (1987).
6. D. A. Darby and J. F. Bischof, *J. Sediment. Petrol.* **66**, 599 (1996). We distinguish between nine black, opaque, magnetic minerals: fresh and altered ilmenite, titanomagnetite, magnetite, magnetite with inclusions, hematite, titanohematite, ferroan ilmenite, and chromite. These minerals were analyzed by electron microprobe for 12 element oxides: TiO₂, FeO, MnO, MgO, SiO₂, Al₂O₃, Cr₂O₃, V₂O₅, ZnO, CaO, Nb₂O₅, and TaO.
7. J. F. Bischof, D. L. Clark, J.-S. Vincent, *Paleoceanography* **11**, 743 (1996).
8. G. H. Denton and T. J. Hughes, Eds., *The Last Great Ice Sheets* (Wiley, New York, 1981); D. Nürnberg *et al.*, *Polar Res.* **14**, 43 (1995); CLIMAP Project Members, *Maps of Northern and Southern Hemisphere Continental Ice, Sea Ice, and Sea Surface Tempera-*

- tures in August for the Modern and the Last Glacial Maximum* (Map and Chart Series MC-36, Geological Society, London, 1981), maps 7A and 7B.
9. D. Hebbeln and G. Wefter, *Nature* **350**, 409 (1991).
 10. E. Reimnitz, P. W. Barnes, W. S. Weber, *J. Glaciol.* **39**, 186 (1993); S. Pirman, I. Wollenburg, P. Goldschmidt, J. Bischof, M. Lange, in *Scientific Cruise Report of Arctic Expeditions ARK VII/1-4 of RV "Polarstern" in 1989*, vol. 87 of *Reports on Polar Research*, G. Krause, J. Meincke, H. J. Schwartz, Eds. (Alfred Wegener Institute for Polar and Marine Research, Bremerhaven, Germany, 1991), pp. 33–35; E. W. Kempema, E. Reimnitz, P. W. Barnes, *J. Sediment. Petrol.* **59**, 308 (1989); E. Kempema, E. Reimnitz, J. Clayton, J. Payne, *Cold Regions Sci. Technol.* **21**, 137 (1993); D. Nürnberg *et al.*, *Mar. Geol.* **119**, 185 (1994).
 11. J.-S. Vincent, in *Quaternary Geology of Canada and Greenland*, R. J. Fulton, Ed. (Geological Survey of Canada, Ottawa, 1989), pp. 100–137.
 12. D. L. Clark and A. Hanson, in *Glacial Marine Sedimentation*, B. F. Molnia, Ed. (Plenum, New York, 1983), pp. 301–330.
 13. D. A. Hodgson, in (11), pp. 442–478; A. S. Dyke, J.-S. Vincent, J. T. Andrews, L. A. Dredge, W. R. Cowan, in (11), pp. 178–189.
 14. B. MacLean *et al.*, *Geol. Surv. Can. Pap.* **89-11** (1989).

15. F. J. Hein, N. A. van Wagoner, P. J. Mudie, *Mar. Geol.* **93**, 243 (1990).
16. D. A. Hodgson, in (11), pp. 452–459.
17. J. E. Kutzbach and P. J. Guetter, *J. Atmos. Sci.* **43**, 1726 (1986); S. Manabe and A. J. Broccoli, *J. Geophys. Res.* **90**, 2167 (1985).
18. A. Y. Proshutinsky and M. A. Johnson, *J. Geophys. Res.*, in press.
19. J. F. Bischof, J. Koch, M. Kubisch, R. F. Spielhagen, J. Thiede, in *Glaciomarine Environments: Processes and Sediments*, J. A. Dowdeswell and J. D. Scourse, Eds. (Geological Society, London, 1990), pp. 235–251.
20. R. Spielhagen, thesis, Kiel University, Germany (1990).
21. R. Stein, H. Grobe, M. Wahsner, *Mar. Geol.* **119**, 269 (1994).
22. N. Untersteiner, in *The Arctic Ocean Region*, vol. 50 of *The Geology of North America*, A. Grantz, L. Johnson, J. F. Sweeney, Eds. (Geological Society of America, Boulder, CO, 1990), pp. 37–51.
23. J. F. Bischof, *Mar. Geol.* **117**, 35 (1994).
24. Supported by NSF grants OPP-9321487 and OPP-9123027 and Office of Naval Research grant N00014-95-1-1200.

15 April 1997; accepted 4 June 1997

Synthesis and Characterization of a Stable Dibismuthene: Evidence for a Bi–Bi Double Bond

Norihiro Tokitoh,* Yoshimitsu Arai, Renji Okazaki,* Shigeru Nagase

Treatment of an overcrowded triselenatribismane, 2,4,6-tris(bis(trimethylsilyl)methyl)phenyl-1,3,5-triseleno-2,4,6-tribismane, with hexamethylphosphorous triamide in toluene at 100°C resulted in the quantitative formation of a stable dibismuthene [TbtBi=BiTbt, where Tbt is 2,4,6-tris(bis(trimethylsilyl)methyl)phenyl], a compound containing a double bond formed between two bismuth atoms. The compound formed as deep purple crystals upon cooling. Ultraviolet-visible and Raman spectra, x-ray crystallographic structural analysis, and theoretical calculations provided evidence for the double bond character of the Bi–Bi bond.

The synthesis of compounds containing double bonds between heavy main group elements has stimulated wide interest (1) because of their unusual structure and properties compared with compounds containing second-row elements, such as olefins (R₂C=CR₂), azo compounds (RN=NR), and ketones (R₂C=O). Several stable compounds with a double bond between heavier group 14 to group 16 elements, such as R₂E=ER₂ [E = Si (2), Ge (3), Sn (4, 5)], RE=ER [E = P (6), As (7)], and R₂E=X (E = Si, Ge; X = S, Se) (8–10), have been synthesized by taking advantage of kinetic stabilization afforded by sterically demanding substituents. Distannenes R₂Sn=SnR₂ have also been syn-

thesized, but they are known to dissociate into the corresponding stannylene R₂Sn: in solution (4, 5, 11). To our knowledge, no stable examples containing sixth-row elements have been reported. Here we report the synthesis of a stable dibismuthene, TbtBi=BiTbt (1), prepared by using an efficient steric protection group 2,4,6-tris(bis(trimethylsilyl)methyl)phenyl (denoted as Tbt hereafter) developed by us (12).

Compound 1 was prepared by deselenation of triselenatribismane 2 with a phosphine reagent. The precursor 2 was readily synthesized (Fig. 1) by nucleophilic substitution of bismuth trichloride with TbtLi, giving the corresponding bismuth dichloride TbtBiCl₂ (3), followed by treatment of 3 with Li₂Se in tetrahydrofuran. Triselenatribismane 2 was isolated as a stable crystalline compound by gel permeation liquid chromatography and was then treated with an excess amount of hexamethylphosphorous triamide in tolu-

N. Tokitoh, Y. Arai, R. Okazaki, Department of Chemistry, Graduate School of Science, The University of Tokyo, 7-3-1 Hongo, Bunkyo-ku, Tokyo 113, Japan. S. Nagase, Department of Chemistry, Faculty of Science, Tokyo Metropolitan University, 1-1 Minami-osawa, Hachioji, Tokyo 192-03, Japan.

*To whom correspondence should be addressed.